LBL-12372
Preprint

Lawrence Berkeley Laboratory

UNIVERSITY OF CALIFORNIA

Materials & Molecular Research Division

To be published as a book chapter in Encyclopedia of Science and Engineering, Pergamon Press, 1982

SURFACE REACTIONS

S.M. Davis and G.A. Somorjai

February 1981

TWO-WEEK LOAN COPY

This is a Library Circulating Copy which may be borrowed for two weeks. For a personal retention copy, call Tech. Info. Division, Ext. 6782

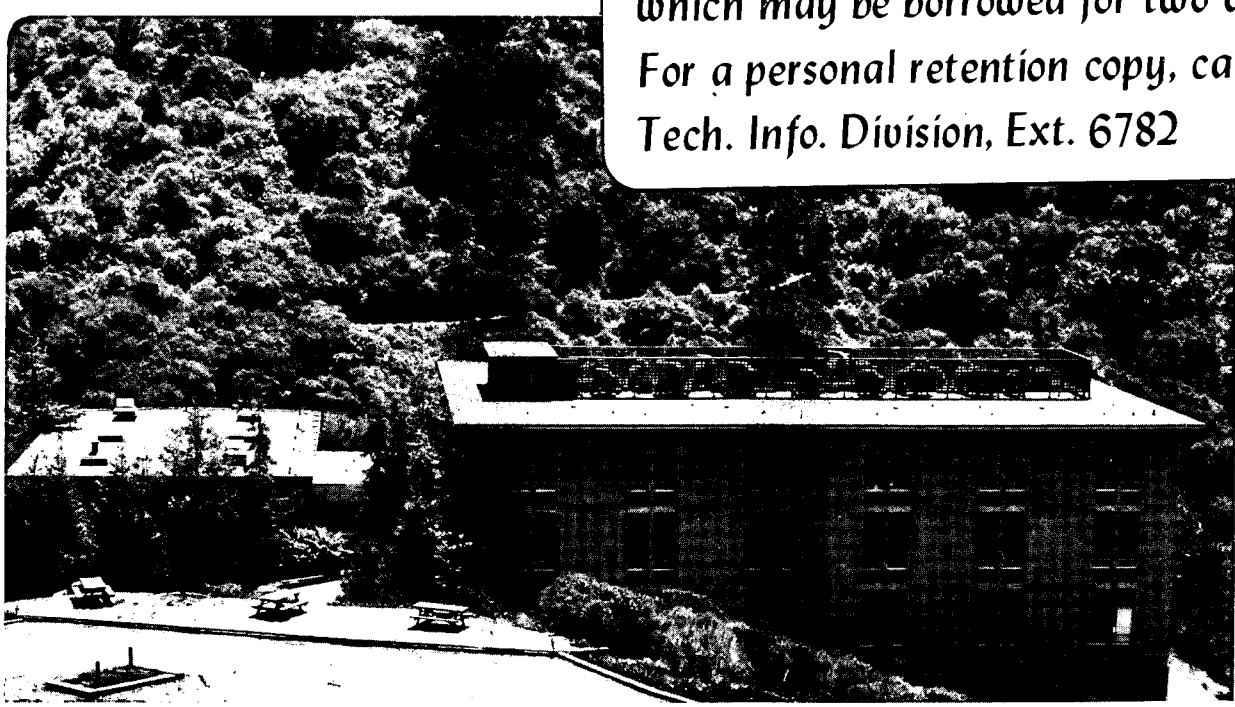

Prepared for the U.S. Department of Energy under Contract W-7405-ENG-48

DISCLAIMER

This document was prepared as an account of work sponsored by the United States Government. While this document is believed to contain correct information, neither the United States Government nor any agency thereof, nor the Regents of the University of California, nor any of their employees, makes any warranty, express or implied, or assumes any legal responsibility for the accuracy, completeness, or usefulness of any information, apparatus, product, or process disclosed, or represents that its use would not infringe privately owned rights. Reference herein to any specific commercial product, process, or service by its trade name, trademark, manufacturer, or otherwise, does not necessarily constitute or imply its endorsement, recommendation, or favoring by the United States Government or any agency thereof, or the Regents of the University of California. The views and opinions of authors expressed herein do not necessarily state or reflect those of the United States Government or any agency thereof or the Regents of the University of California.

LBL 12372

SURFACE REACTIONS

S.M. Davis and G.A. Somorjai

Materials and Molecular Research Division,
Lawrence Berkeley Laboratory, and Department of Chemistry,
University of California, Berkeley, CA 94720

This work was supported by the Director, Office of Energy Research,
Office of Basic Energy Sciences, Materials Science Division of the U.S.
Department of Energy under Contract Number W-7405-ENG-48

Surface reactions formally encompass all chemical reactions which occur at an interface between distinguishable phases of matter. Adhesion, corrosion, photosynthesis, and heterogeneous catalysis are a few examples of essential chemical phenomena that are partially or entirely controlled by reactions at surfaces. In this chapter we shall concentrate on surface ractions which occur at the gas-solid interface. In this instance, the termination of the solid constitutes the surface, and reactions take place between adsorbed species which exist in quasiequilibrium with the gas phase. These surface reactions can be divided into two main categories: (1) the solid surface particpates directly in the reaction by compound formation,

$$S_s + A_g \longrightarrow SA_g \text{ or } SA_s$$

or, (2) reaction occurs under the catalytic influence of the solid surface, but the surface undergoes no net chemical change,

$$A_g + B_g \xrightarrow{s} AB_g$$

The first class of reactions corresponds to the initial stages of solid state reactions that are of paramount importance in corrosion science. Chemical and petroleum technologies based on heterogeneous catalysis utilize the second category of surface reactions. Both types of reactions take place under conditions of atom transport. Gaseous molecules impinge, adsorb, react on the surface, form intermediates of various lifetimes, then the products desorb into the gas phase, except when the product is non-volatile.

Emphasis is focussed here on the investigation of surface reaction dynamics from the perspective of surface science. In the first section we summarize essential elementary concepts of adsorption and surface reaction

kinetics. The second section considers in more detail the molecular dynamics of simple catalyzed surface reactions which were derived from molecular beam reactive scattering studies. In the third section we turn to a brief discussion of oxidation and related surface reactions that are important in materials science and engineering. We conclude with an introduction to the chemistry and concepts of catalytic processes.

1. Elementary Concepts

All surface reactions involve a sequence of elementary steps that begin with the colision of incident atoms or molecules with the surface. As the gas species approaches the surface, it experiences an attractive potential whose range and strength depend on the atomic and electronic structures of the gas and surface atoms. This gas-solid interaction potential may be of long range and vary in proportion to the reciprocal of the distance between the gas molecule (or ion) and the surface (Coulombic interaction). It may be of much shorter range and vary in proportion with the inverse third or sixth powers of the distance (ion-dipole and dipole-dipole interactions). A certain fraction of the incident gas molecules is trapped in this attractive potential well with a sticking probability given by

$$S(\Theta,T) = S_o(1-\Theta)\exp(-E_a/RT) \qquad (1)$$

where S_o is the initial (zero coverage) sticking coefficient, Θ is the surface coverage ($o < \Theta < 1$), and E_a is the activation energy for adsorption. Once trapped, the adsorbed molecules can move along the surface by diffusion. The adsorbed species may desorb from the surface if sufficient energy is imparted to it at a given site to overcome the attractive surface forces. When a surface reaction occurs, a certain fraction of the adsorbed species re-

arranges, decomposes (unimolecular reactions), or reacts with a second adsorbed species (bimolecular reactions) before desorption takes place.

During the collision of the gas molecule with the surface it exchanges translational energy, T, with the vibrational modes (phonon states), V_S, of the surface atoms. This type of energy transfer is callted $T-V_S$ energy exchange. The gas moleucles may also exchange internal energy, rotation, R, or vibration, V, wth the vibrating surface atoms. In this case, $R-V_S$ and $V-V_S$ energy transfer channels also exist.

Most surface reactions take place at high pressures (1-100 atmospheres) either because of the chemical environment of our planet or to establish optimum reaction rates in chemical processing. Under these conditions, surfaces are usually covered by at least one monolayer of adsorbed species (2). Since activation energies for adsorption and surface diffusion are generally small (a few kT), equilibrium among the different surface species, reactants, reaction intermediates, and products, is readily established. In the simplest (but most general and important) case of localized, <u>associative</u> adsorption into a single state, the surface coverage by adsorbed species is given in terms of the gas pressure, P, by the Langmuir isotherm (3)

$$\Theta = KP/(1 + KP) \qquad (2)$$

The adsorption equilibrium constant, K, has the general form

$$K = \frac{S_o}{\nu_o(2\pi mkT)^{\frac{1}{2}}} \exp\left[(E_d - E_a)/RT\right] \qquad (3)$$

Where ν_o and E_d are the coverage dependent pre-exponential factor and activation energy for desorption, respectively. Typically, E_d decreases with increasing coverage ($E_d(\Theta) \simeq E_d^o - \alpha\Theta$), and $E_d - E_a$ represents the heat of adsorption (4). When a gas molecule <u>dissociates</u> into n equivalent

adsorbed species (5) the coverage is given by

$$\theta = (KP)^{1/n} / (1 + (KP)^{1/n}) \qquad (4)$$

Catalyzed surface reactions usually take place between two or more coadsorbed species which compete for adsorption sites on the surface. When j gases adsorb competitively and associatively, the surface coverage by species i is given by (5)

$$\theta = K_i P_i / (1 + \Sigma_j K_j P_j) \qquad (5)$$

Many catalyzed surface reactions can be treated as a two-step process with an adsorption equilibrium followed by one rate-determining step (diffusion, surface reaction, or desorption)(6). The surface reaction kinetics are usually discussed in terms of two limiting mechanisms, the Langmuir-Hinshelwood (LH) and Eley-Rideal (ER) mechanisms (7). In the LH mechanism, reaction takes place directly between species which are chemically bonded (chemisorbed) on the surface. For a bimolecular LH surface reaction, $A_{ads}+B_{ads}$-> products, with competitive chemisorption of the reactants, the rate of reaction, ν_R, is given by the expression (7)

$$\nu_R = k_R \theta_A \theta_B = k_R K_A K_B P_A P_B / (1+K_A P_A + K_B P_B)^2 \qquad (6)$$

The reaction rate is proportional to the surface coverages θ_A and θ_B and to the reaction rate constant k_R. For non-competitive adsorption, the rate expression becomes

$$\nu_R = k_R \theta_A \theta_B = k_R K_A K_B P_A P_B / (1+ K_A P_A)(1+ K_B P_B) \qquad (7)$$

General rate expressions of the form given in equations 6 and 7 have been experimentally verified for many types of LH reactions (6,8). Similar but more complicated rate expresssions are easily derived assuming different (non-Langmuir) isotherms, higher order reaction steps, or dissociative chemisorp-

tion of the reactans. In the ER mechanism, surface reaction takes place between a chemisorbed species and a non-chemisorbed species, e.g. $A_{ads}+B_g \rightarrow$ products. The non-chemisorbed species may be physisorbed or weakly held in a molecular precursor state (9). In this case, the rate expression for the surface reaction becomes

$$\nu_R = k_R\Theta_A P_B = k_R K_A P_A P_B / (1+K_A P_A) \qquad (8)$$

Presently no proven examples exist in which surface reaction occurs by the ER mechanism. Rate expressions of the form given in equation 8 can also be obtained with LH mechanisms provided that species A is more strongly adsorbed than species B.

Surface reaction kinetics determined experimentally are often expressed in the form of a power rate law (6),

$$\nu_R = k_R \Pi_i P_i^{\alpha_i} \qquad (9)$$

where k_R is the apparent rate constant and the α_is are the experimental orders of the reaction (positive, negative, integer, or fraction) with respect to i reactants and products. The apparent rate constant in equation 9 is not that of an elementary reaction step (it contains adsorption equilibrium constants), but it can usually be represented by an Arrhenius equation,

$$k_R = A\exp(-E_R/RT) \qquad (10)$$

where A is an apparent pre-exponential factor and E_R is the apparent activation energy for the surface reaction. The magnitude of A and E_A can provide important information about the rate determining step of a surface reaction (10), and very frequently, k_R and A display a compensation effect (11). A related quantity is the <u>reaction probability</u>, $\gamma_i=(2\pi mKT)^{\frac{1}{2}}\ \nu_R/P_i=$ rate/flux, that is, the probability that an incident reactant molecule will undergo reaction.

The simplified isotherms and rate expressions developed in this section are extremely useful despite the implicit assumption that a single state exists for the adsorbed species. Real surfaces are heterogeneous on an atomic scale with a variety of distinguishable adsorption sites. Gas molecules adsorbed at each type of site may display a wide distribution of excited rotational, vibrational, and electronic states. Experimentally, one can measure meaningful rate and adsorption equilibrium constants provided that adsorption and desorption are fast compared with surface reactions so that an adsorption equilibrium exists. In this circumstance the kinetic parameters are an ensemble average over all surface sites and states of the system, e.g.,

$$\text{Rate} \equiv \sum_{\text{sites}} \sum_{\text{states}} \nu_R \Big/ \sum_{\text{sites}} \sum_{\text{states}} \qquad (11)$$

Theoretical studies of the state-to-state dependence of the reaction rates and reaction probabilities are still in their infancy (12).

2. Molecular Beam Scattering Studies of Surface Reaction Dynamics

Explosive development of surface science during the past two decades has provided detailed information about the dynamics of gas-solid interactions (13). Surface reactions can be carefully investigated over a wide range of pressure ($\approx 10^{-10}$-10^{-2} atm) on small area single crystal surfaces with uniform atomic surface structure and composition (14). The structure, bonding, and residence times of adsorbed reactants, intermediates, and products are characterized *in situ* using an extensive arsenal of surface analysis techniques (13,15). These studies have revealed the special importance of *surface structure* and *surface additives* in controlling the kinetics and mechanisms in a variety of important surface reactions (13,16). The paramount objective of these surface science studies is to understand on an atomic scale how surfaces lower the activation energy for chemical reactions so that they proceed readily, while the same

reactions in the gas phase are highly improbable.

Molecular beam reactive scattering (MBRS) has emerged as the most powerful experimental technique for investigating the dynamics of the gas-solid interaction (13,17). A schematic diagram of MBRS is shown in Figure 1a. Under single scattering conditions at low reacxtant pressures ($<10^{-6}$ atm), a collimated beam of atoms or molecules strike an oriented (preferably single crystal) surface, and the species that are desorbed at a specific solid angle are detected with a mass spectrometer. If the incident beam is chopped at well defined frequencies, the time-of-flight of the incident molecules between the chopper and detector can be deduced from phase shift measurements (18). The phase lag yields the residence times of the reacting molecules on the surface (13,19). Chopping the product molecules which desorb from the surface permits determination of their time-of-flight and translational energy distributions (20). Activation energies for adsorption and surface reactions are determined by varying the incident beam velocity (temperature) and surface temperature, respectively. The angular distribution for the desorbing products is measured by rotating the mass spectrometer around the oriented sample. The surface residence times of the molecules together with their angular and kinetic energy distributions provide detailed information about the $T-V_S$ energy tranfer processes that occur during the gas-surface interaction. Complete dynamical description for this interaction ($T-V_S$ plus $R-V_S$ and $V-V_S$) can be realized if the distribution of internal energy states for the product molecules is determined simultaneously with their velocity distributions (21). While little is now known about the $V-V_S$ interaction, existing information (13,22) indicates $R-V_S$ energy transfer is efficient provided that the rotational energy levels overlap the phonon spectrum of the solid.

The angular distribution of scattered molecules is usually displayed by

plotting the intensity (number density) of detected molecules per unit solid angle versus the angle of scattering Θ_r, that is measured with respect to the surface normal (rectilinear plot). Angular distributions in the two limiting cases of gas-surface interaction, cosine and specular scattering, are shown in Figure 1b. The angle of incidence (45°) is indicated by the arrow. The scattered intensity for the cosine distribution decreases as cos Θ with respect to the surface normal. Cosine scattering is expected when the adsorbed species have long residence times, or strongly couple with the vibrational states of the surface atoms. A cosine scattering distribution is a necessary criterion for complete thermal accomodation, a situation in which the molecules desorb with kinetic temperature or velocity distribution that is the same as the temperature of the solid surface (23). Specular scattering occurs when the scattered intensity is sharply peaked at the angle of incidence (specular angle). In this case the interaction is elastic or quasi-elastic and little or no energy tansfer takes place between the incident gas molecules and the surface (24). Sharply peaked angular distributions for surface reaction products ($I(\Theta) \sim \cos^m\Theta, m>1$) indicate that a repulsive barrier exists in the exit product moelcules usually desorb with a kinetic temperature that is higher than that of the surface. Direct measurement of the velocity distribution of the product molecules helps to quantify the extent of $T-V_s$ energy transfer along the exit channel of the potential energy surface (25).

Molecular beam reactive scattering was used to investigate the dynamics of several small molecule and atom recombination reactions catalyzed on clean metal surfaces (17,18). The oxidation of CO ($CO+1/2O_2 \rightarrow CO_2$) (26,27), H_2-D_2 exchange ($H_2+D_2 \rightarrow 2HD$) (28,29), the oxidation of D and D_2 ($D_2+1/2O_2 \rightarrow D_2O$)

(30,31), and ammonia decomposition ($NH_3 \rightarrow 1/2\ N_2 + 3/2\ H_2$) (32) catalyzed over clean platinum surfaces are considered here as examples. Similar results were obtained for the H_2-D_2 and H_2-O_2 reactions catalyzed on palladium (33,34).

At temperatures between 400 and 700 K, CO oxidation follows an LH mechanism in which chemisorbed CO molecules react with unit reaction probability with chemisorbed oxygen atoms (26). This reaction displays an activation energy of 100 kJ/mole when both species are present at low coverage. Because of repulsive interactions between oxygen adatoms, this activation energy decreases to about 50 kJ/mole at high oxygen coverages. The angular distribution for the product CO_2 molecules varies from $\cos\theta$ to $\cos^6\theta$ with increasing temperature and increasing coverage by oxygen and CO. The sharply peaked $\cos^6\theta$ angular distributions are an indication that the CO_2 product is desorbed with excess translational energy. This was confirmed by velocity distribution measurements when the surface temperature was 880 K (27). At the surface normal (0°), the kinetic tempeature of the CO_2 molecules was 3600 K, while at 45° it was 2100 K. These high kinetic temperatures indicate that 5-10% of the exothermic reaction energy ($\Delta H = -286$ kJ/mole) was converted into translational energy of the reaction products. The most energetic molecules exit normal to the surface.

Exchange of hydrogen and deuterium to form hydrogen deuterium, HD, is one of the simplest reactions that can be catalyzed on clean metal surfaces at temperatures as low as 100 K. The same reaction is immeasurably slow in the gas phase because of the large dissociation energies (436 kJ/mole) of the reacting molecules. The H_2-D_2 exchange reactions was studied over flat (111) and "stepped" (332) single crystal surfaces of platinum. The latter contains high concentrations of periodic surface irregularities (steps) that are one atom

in height. Reaction probabilities averaged over the cosine HD angular distributions were 0.07 on the (111) surface and 0.35 on the (332) surface under identical experimental conditions (T_s=1100 K, T_g=300 K) (28). The reaction probability on the stepped surface varied markedly with the angle of incidence of the mixed H_2-D_2 molecular beam. This is shown in Figure 2. The reaction probability was highest when the beam was incident upon the open edge of the step and lowest when the bottom of the step was shadowed (curve a). When the H_2-D_2 beam was incident parallel to the steps, the rate of HD production was independent of the angle of incident at all angles of crystal rotation (curve b). These results indicate that the atomic step sites are about seven times more active than the (111) terrace sites for the dissociative chemisorption of hydrogen and deuterium molecules. Detailed analysis of the scattering data (29) revealed a barrier height of 4-8 kJ/mole for dissociative H_2 chemisorption on the (111) surface. On the other hand, this barrier did not exist (E_a=0) on the stepped surface. This difference in activation energy alone accounts for the different reaction probabilities of the step and terrace sites. While the dissociation probability of hydrogen molecules was higher on the stepped surface than on Pt(111), the kinetics and mechanism of HD recombination appear to be identical over both surfaces once dissociation takes place. On both surfaces, HD formation follows a parallel LH mechanism with one of the reaction branches operative over the entire temperature range of 300-1075 K. This branch has an activation energy and pseudo-first-order pre-exponential factor of E_a=54 kJ/mole and A_1=8x10^{4}sec^{-1} for the stepped surface, and E_a=65 kJ/mole and A_1=3x10^{5}sec^{-1} for the Pt(111) surace. A second branch is observed for temperatures above 575 K, but the kinetic parameters for this pathway could not be accurately determined.

The angular distributions of D_2O molecules produced from the reactions

of D and D_2 with O_2 at 425-850 K are both cosine (30,31). The D_2-O_2 reaction displays an activation energy of 50 kJ/mole with mean reaction times ranging from 10^{-2} to 10^{-4} sec (31). In the D+O_2 reactions, incident deuterium atoms are trapped at the surface and thermally equilibrate before reaction takes place by an LH mechanism (30). From the energetics shown in Figure 3, the lowest energy pathway involves combination of deuterium and oxygen atoms to form intermediate OD species followed by deuterium addition to produce adsorbed D_2O. An alternate pathway (also shown in Fig.3) involves recombination of deuterium atoms followed by oxygen insertion into adsorbed D_2. This mechanism appears to be energetically less favorable because of the repulsive barrier (28) which exists for dissociative chemisorption of $D_2(H_2)$ on Pt(111).

Ammonia adsorption, desorption, and decomposition on (111) and stepped (557) platinum surfaces was also studied by MBRS (32). Ammonia adsorbed associatively on both surfaces at 300-400 K with a sticking coefficient near unity and residence times of 10^{-2}-1 sec. Desorbing ammonia molecules displayed a cosine angular distribution with a desorption activation energy of 64 kJ/mole. Decomposition to nitrogen and hydrogen occurred between 600 and 750 K with an activation energy of 75$\pm$5 kJ/mole. The maximum reaction probability for decomposition was 0.18 at 750 K on Pt(557). Step sites on the (557) platinum surface were at least 16 times more active than (111) terrace sites for the decomposition reaction. A kinetic model for the reaction involving stepwise decomposition of adsorbed ammonia (NH_3—>NH_2—>NH—>N) with rapid recombination of hydrogen atoms and slower recombination of nitrogen gave good agreement with the experimental results.

3. Oxidation, Corrosion, and Related Surface Reactions

Surface oxidation of metals encompasses a series of at least three reaction steps that include (1) dissocative chemisorption of oxygen on the metal surface, (2) rearrangement of the surface atoms with dissolution of oxygen into the near surface region, and (3) nucleation of oxide islands which grow laterally and eventually condense to produce continuous oxide films (35). The oxide islands appear to precipitate suddenly once a critical oxygen concentration is reached in the near surace region. Nucleation takes place most readily at surface irregularities such as atomic steps, dislocations, and stacking faults. At room temperature, noble metals such as Rh, Ir, Pd, and Pt display little tendency for oxygen incorporation or surface rearrangement. Initial heats of oxygen chemisorption on these metals are much greater than the heats of formation of the corresponding bulk oxides (36). Other metals such as Cr, Nb, Ta, Mo, W Re, Ru, Co and Ni, dissolve surface oxygen by a place exchange mechanism where oxygen atoms interchange positions with underlying metal atoms. Thse metals display heats of adsorption for oxygen that are comparable to the heats of formation of the stable metal oxides (36). Metals such as Ti, Zr, Mn, Al, Cu, and Fe dissolve oxygen more readily and form stable oxide films even at room temperature. At low oxygen pressures these films often assume a crystalline structure, whereas at higher pressures ($>10^{-3}$ atm) the films tend to be amorphous (35). At higher temperatures (400-1000 K), oxide formation occurs readily on the surfaces of nearly all metals.

Growth of surface oxide films takes place only if cations, anions, and electrons can diffuse through the oxide layer. The growth kinetics of very thin films (~10-50 Å) often follows the Mott (37) or Cabrera-Mott (38)

mechanisms in which electrons tunnel through the film and assocaite with oxygen atoms to produce oxide ions at the surface. A large local electric field (10^6-10^7 V/cm) results at the surface which facilitates cation diffusion from the metal-oxide interface to an interstitial site of the oxide. The film thickness, Z, at time, t, is given by a logarithmic,

$$Z = \alpha_1 \ln(\alpha_2 t+1) \tag{12}$$

or inverse logarithmic

$$1/Z = \alpha_3 - \alpha_4 \ln t \tag{13}$$

law of growth depending upon whether electron tunneling or cation diffusion is rate limiting. The constants $\alpha_1 - \alpha_4$ are determined by the material, its structure, and the reaction conditions. The electric field strength and rate of growth decrease exponentially as the film thickens, thereby resulting in an effective limiting thickness for the surface oxide layer.

In addition to surface oxides, a vast array of surface compounds can be produced from the reactions of halogen, chalcogenides, and carbon-containing molecules with metal surfaces. Chemisorption of chlorine near 300 K on Cu (39), Ti (40), W (41), Mo (42), Ta (43), Ni (44), Pd (45), and Au (46), for example, results in the formation of stable surface compounds which often evaporate as molecular chlorides upon heating at elevated temperatures. Chemisorption of chlorine at 300 K on Ag(100) and Ag(111) produces chemisorbed chlorine overlayers which react irreversibly at about 425 K to produce AgCl with an activation energy of 56 kJ/mole (47,48). Upon heating, AgCl desorbs at about 820 K with a desorption activation energy of 192 kJ/mole (48).

Chemisorption of H_2S or S_2 on transition metal surfaces near 300 K produces strongly adsorbed sulfur overlayers with unique chemical stability. These overlayers display heats of adsorption that are typically 20-40%

higher than the corresponding heats of formation of bulk sulfides (49). The heat of adsorption gradually approaches the bulk sulfide enthalpy of formation as the sulfur coverage approaches one monolayer. This is accompanied by major restructuring within the surface layer and/or surface compound formation (sulfidization). Sulfur adsorption at 300 K on Ag(111), for example, leads initially to a complex compound identifiable with the (100) plane of $-Ag_2S$ (50). Multilayer growth is accompanied by further restructuring to a compound with properties identical to the (111) plane of Ag_2S. Two-dimensional surface sulfides have also been characterized for Cu (51), Ni (52), Fe (53), Pb (54), and Au (53). Decomposition of these compounds upon heating at elevated temperatures causes sulfur diffusion into the near surface region with an activation energy that is close to that for self-diffusion of the metal (49).

Carbon containing molecules react at elevated temperatures (450-1000 K) with iron and most early transition metals (viz. Ti, Zr, Hf, V. Nb, Ta, Cr, Mo, W) to form surface carbides (carbidization) which display complex surface structures and non-stoichiometric composition (MC_x, $x \approx 0.5-0.95$) (56). Presently, very little is known about these compound formation reactions.

Molecular beam reactive scattering was used to investigate the dynamics of several surface corrosion reactions at low reactant pressures. Systems studied include the oxidation Si (57), Ge (58), Mo (59), and graphite (60), and the halogenation of Si (61), Ge (62), Ta (63), and Ni (64). With the exception of silicon and germanium oxidation, where dissociative chemisorption of oxygen is apparently rate-limiting, the kinetics of these surface rections generally appear to be controlled by surface or bulk diffusion of the reacting species (as indicated by the small activation energies at pre-exponential

factors). Diffusion limitation of the reaction rates at low pressures can sometimes arise as an artefact of the modulated beam flux since the surface does not hae a constant equilibrium supply of reactant (17). The reaction of chlorine with nickel at 1000 K produces NiCl and $NiCl_2$ with a total reaction probability of about 0.8 (64). Formation of NiCl prevails at low temperatues (<1000 K), while $NiCl_2$ forms almost exclusively above 1400 K. The formation of an Ni_2Cl_2 surface intermediate appears to be the rate-limiting step of the reaction. The surface residence times of desorbing NiCl varies from 900 μ sec at 1450 K to 140 μ sec at 1700 K, and the $NiCl_2$ residence times are even longer.

4. Heterogeneous Catalysis at Higher Pressures

Molecular beam scattering studies are ideally suited for detailed understanding of energy transfer processes that take place during surface reactions at low pressures. Unfortunately, these studies are far removed from the reaction conditions utilized in practical catalysis. Commercial catalytic processes are carried out at pressures of 1-100 atm in order to obtain maximum reaction rates and equilibrium conversions. The catalysts usualy consist of microcrystallites $10-10^4$ Å in diameter of an active component dispersed on a porous, high surface area support (carbon, silica, alumina). These 'supported' catalysts provide a maximuma active surface area per unit weight of catalyst (typically $10-10^3 m^2/g$) (65).

The most important catalytic processes are summarized in Table I (66). These processes are listed together with the pertinent chemical reactions, widely used catalysts, and typical process conditions. Transition metals of Group VIII and transition metal oxides are the preferred catalysts for most of these processes, especially those involving dehydrogenation (14), reduction (66), or oxidation (66). Skeletal rearrangement of hydrocarbons

readily takes place by carbonium ion mechanisms over solid acid and zeolite catalysts (67).

Several definitions are appropriate to place in context the language and terminology of heterogeneous catalysis. Catalytic activity is the rate of a catalyzed surface reaction expressed as reactant molecules converted per unit area of catalyst per unit time, e.g. molec/cm^2sec. Acivities are frequently expressed as rates per exposed surface atom or turnover frequencies. Dispersion is defined as the fraction of total catalyst atoms which are exposed at the surface. Catalytic selectivity expresses the tendency for one reaction product to the produced over all others. Selectivity is usually defined as the proportion of the reaction leading to a specific product (fractional selectivity = $\nu / \Sigma_i \nu_i$) or as a simple ratio of reaction rates for competing reaction pathways (kinetic selectivity = $\nu_i \nu_k$). High catalytic specificity represents a unique combination of high activity and selectivity.

Most catalysts contain a complex mixture of chemical additives or modifiers that are essential ingredients for high activity and selectivity. Promoters are beneficial additives that increase activity, selectivity, or useful catalyst lifetime (stability). Structural promoters inhibit sintering of the active catalyst phase or prevent compound formation between the active component and the support. Halogens, alkali metals, and chalcogenides are common chemical promoters. Poisons are undesirable additives which cause surface restructuring or block sites so as to render the catalyst inactive. Selective poisons enhance selectivity by blocking only those sites which are required for unwanted side reactions.

Turnover frequencies at high pressures for most of the important catalyzed reactions vary from 10^{-4} to 10^{2} molec/site sec. Therefore, the reaction probabilities are very small, typically 10^{-14} - 10^{-6} (14). At the higher

pressures, most of the incident molecules scatter or desorb from the surface without undergoing any chemical reaction because the adsorption sites, where chemical rearrangement takes place, are completely, and effectively continuously, occupied by adsorbed species. The mean residence times of these species (typically 10^{-4}-1 sec) are very long compared to the period between collision of incident gas molecules ($\sim 10^{-12} - 10^{-10}$ sec at a given atomic site).

Finally, we note that certain thermodynamically 'uphill' ($\Delta G > 0$) surface reactions can be forced to occur under the catalytic influence of photon illumination. Perhaps the most important of these photoassisted reactions is the photocatalytic decomposition of water ($H_2O \xrightarrow{h\nu} 1/2O_2 + H_2$). This reaction occurs readily at metal-semiconductor interfaces in the presence of band-gap radiation (68).

Acknowledgement: This work was supported by the Director, Office of Energy Research, Office of Basic Energy Sciences, Materials Sciences Division of the U.S. Department of Energy under Contract W-7405-ENG-48.

References

1. D.A. King, CRC Crital Rev. Solid State Mater. Sci. 7, 617 (1978); Ch. Steinbruchel and L.D. Schmidt, J. Vac. Sci. Technol. 12, 204, (1975).

2. G.A. Somorjai, Principles of Surface Chemistry, Prentice-Hall, Englewood Cliffs, NJ, 1972.

3. I. Langmuir, J. Amer. Chem. Soc. 40, 1361 (1918).

4. M.W. Roberts and C.S. McKee, Chemistry of the Metal-Gas Interface, Oxford Press, Oxford, 1978.

5. J.M. Thomas and W.J. Thomas, Introduction to the Principles of Heterogeneous Catalysis, Academic Press, New York, 1967.

6. M. Boudart, Amer. Inst. Chem. Eng. J. 18, 465 (1972).

7. A. Clark, The Theory of Adsorption and Catalysis, Academic Press, New York, 1970; E.K. Rideal, Concepts in Catalysis, Academic Press, New York, 1968; L.D. Schmidt, J. Vac. Sci. Technol. 12, 341 (1975).

8. G.C. Bond, Catalysis by Metals, Academic Press, New York, 1962; K. Laidler, J. Catal. 1, 119, (1961).

9. A. Cassuto and D.A. King, Surface Sci. 102, 388 (1981); P. Kisluik, J. Phys. Chem. Solids 5, 78 (1958); R. Gorte and L.D. Schmidt, Surface Sci. 76, 559 (1978).

10. R.C. Baetzold and G.A. Somorjai, J. Catal. 45, 94 (1976).

11. A.K. Galwey, Adv. Catal. 26, 2907 (1977).

12. T.B. Grimley and J.R. Smith, Critical Issues (Theory) in, The Physical Basis for Heterogeneous Catalysis, Plenum Press, New York, 1975.

13. G.A. Somorjai, Chemistry in Two Dimensions: Surfaces, Cornell University Press, Ithaca, New York, 1981.

14. S.M. Davis and G.A. Somorjai, Hydrocarbon Conversion over Metal Catalysts, in The Chemical Physics of Solid Surfaces and Heterogeneous Catalysis, Elsevier, Amsterdam, 1981; T. Engel and G. Ertl. Adv. Catal. 28, 1, 1979

15. G.Ertl and K. Kuppers, Low Energy Electrons and Surface Chemistry, Verlag Chemie, 1974; R.B. Anderson, Experimental Methods in Catalytic Research, Vols.1-3, Academic Press, New York, 1968-1976; W.M. Delgass, G.L. Haller, R. Kellerman, and J.H. Lunsford, Spectroscopy in Heterogeneous Catalysis Academic Press, New York, 1979.

16. G.A. Somorjai, Surface Sci. 89, 496 (1979).

17. S.T. Ceyer and G.A. Somorjai, Ann. Rev. Phys. Chem. 28, 477 (1977).

18. R.H. Jones, D.R. Olander, W.J. Siekhaus, and J.A. Schwarz, J. Vac. Sci. Technol. 9, 1429 (1972).

19. J.A. Schwarz and R.J. Madix, Surface Sci. 46, 317 (1974); G. Ertl, Surface Sci. 89, 525 (1979); H.C. Chang, and W.H. Weinberg, Surface Sci. 72, 617 (1978).

20. V.L. Hirschy and J.P. Aldridge, Rev. Sci. Instr. 42, 381 (1971).

21. F. Frenkel, J. Hager, W. Krieger, H. Walther, C.T. Campbell, G. Ertl, H. Kuipers, and J. Segner, Chem. Phys. Lett, in press; G.M. McClelland, G.D. Kubiak, H.C. Rennagel, and R.N. Zare, J. Chem. Phys. in press.

22. S. Bernasek and G.A. Somorjai, J. Chem. Phys. 62, 3149 (1975); R. Palmer, H. Saltsburg, and J. Smith, J. Chem. Phys. 50, 4661 (1969).

23. L. Thomas, in Fundamentals of Gas-Surface Interactions, Academic Press, New York, 1967, p.346.

24. W.H. Weinberg and R.P. Merrill, J. Chem. Phys. 56, 2881 (1972); R. Sau and R.P. Merrill, Surface Sci. 34, 268 (1973).

25. J.H. McCreery and G. Wolken, Jr., J. Chem. Phys. 65, 1310 (1976); F.O. Goodman, Surface Sci. 30, 525 (1972).

26. C.T. Campbell, G. Ertl, H. Kuipers, and J. Segner, J. Chem. Phys. 73, 5862 (1980).

27. C.A. Becker, J.P. Cowin, L. Wharton, and D.J. Auerbach, J. Chem. Phys. 67, 3394 (1977).

28. R.J. Gale, M. Salmeron, and G.A. Somorjai, J. Chem. Phys. 67, 5324 (1977).

29. M. Salmeron, R.J. Gale, and G.A. Somorjai, J. Chem. Phys. 70, 2807 (1979).

30. S.T.Ceyer, Ph.D. Thesis, University of California, Berkeley, 1979.

31. J.N. Smith Jr., and R.L. Palmer, J. Chem. Phys. 56, 13 (1972).

32. W.D. Guthrie, J.D. Sokol, and G.A. Somorjai, Surface Sci., in press.

33. T. Engel and H. Kuipers, Surface Sci. 90, 162 (1979).

34. R. Engel and H. Kuipers, Surface Sci. 90, 181 (1979).

35. K.R. Lawless, Rep. Prog. Phys. 37, 231 (1974).

36. D.O. Hayward, in Chemisorption and Reactions on Metallic Films, Academic Press, New York, 1971, p. 226; I Toyoshima and G.A. Somorjai, Catal. Rev. 19, 150 (1979).

37. N.F. Mott, Proc. Roy. Soc. A 171, 944 (1939); N.F. Mott, Trans. Faraday Soc. 43, 429 (1947).

38. N. Cabrera and N.F. Mott, Rep. Prog. Phys. 12, 163 (1949).

39. J.P. Goddard and R.M. Lambert, Surface Sci. 67, 180 (1977).

40. I.H. Khan, Surface Sci. 48, 537 (1975).

41. G.G. Price, K.J. Rawlings, and B.J. Hopkins, Surface Sci. 85, 379 (1979).

42. R.G. Jones and D.L. Perry, Surface Sci. 88, 331 (1979).

43. J.Y. Caradac, J.L. Philippart, B. Weber, and A. Cassuto, Surface Sci. 54, 593 (1976).

44. W. Erley and H. Wagner, Surface Sci. 66, 371 (1977).

45. K. Kishi and S. Ikeda, J. Phys. Chem. 78, 107 (1974).

46. W.T. Tysoe and R.M. Lambert, Surface Sci., in press.

47. M. Kitson and R.M. Lambert, Surface Sci. 100, 368 (1980).

48. N.D. Spencer and R.M. Lambert, Surface Sci., in press.

49. J. Oudar, Catal. Rev. 22, 171 (1980).

50. K. Schwaha, N.D. Spencer and R.M. Lambert, Surface Sci. 81, 273 (1979).

51. J.L. Domange and J. Oudar, Surfce Sci. 11, 124 (1968).

52. M. Perdereau and J. Oudar, Surface Sci. 20, 80 (1970).

53. E. Margot, J.Oudar, and J. Benard, Compt. Rend. C270, 1261 (1970).

54. R.W. Joyner, K. Kishi, and M.W. Roberts, Proc. Roy. Soc. A 358, 223 (1977).

55. M. Kostelitz and J. Oudar, Surface Sci.27, 176 (1971).

56. W.S. Williams, Prog. Soid State Chem. 6, 57 (1971).

57. R.J. Madix, R. Parks, A.A. Sasu, and J.A. Schwarz, Surface Sci. 24, 288 (1971).

58. R.J. Madix and A.A. Sasu, Surface Sci. 20, 377 (1970).

59. R.J. Madix and A.Z. Ullman, High Temp. Sci. 6, 342 (1974).

60. D.R. Olander, W. Siekhaus, R.Jones, and J.A. Schwarz, J. Chem. Phys. 57, 408 (1972).

61. R.J. Madix and A.A. Sasu, J. Catal. 28, 408 (1972).

62. R.J. Madix and A.A. Sasu, J. Vac. Sci. & Technol. 9, 915 (1972).

63. A. Machiels and D.R. Olander, Surface Sci. 65, 325 (1977).

64. J. McKinley, J. Chem. Phys. 40, 120 (1964).

65. B. Delmon, P. Jacobs, and G. Poncelot, Preparation of Catalysts, Vols. 1-3, Elsevier, 1975-78.

66. B.C. Gates, J.R. Katzer, G.C.A. Schuit, Chemistry of Catalytic Processes, McGraw-Hill, 1979; P.H. Emmett, Catalysis, Vols.1-7 Reinhold, New York, 1954.

67. J.A. Rabo, Zeolite Chemistry and Catalysis, ACS Monograph 17, Washington, 1976.

68. M.S. Wrighton, Interfacial Photoprocesses: Energy Conversion and Synthesis, Adv. in Chem. 184, ACS, Washington, 1980.

Figure Captions

Figure 1. (a) Scheme of the molecular beam-surface scattering experiment; (b) Angular distributions in the two limiting cases of specular (curve a), and cosine scattering (curve b).

Figure 2. The reaction probability to produce H-D upon single scattering of a mixed H_2-D_2 molecular beam on a stepped platinum single crystal surface as a function of the angle of incidence: (a) the step edges are perpendicular to the incident beam, (b) the projection of the beam on the surface is parallel to the step edges.

Figure 3. Reaction coordinate showing the energetics of the D_2-O_2 reaction on Pt(111).

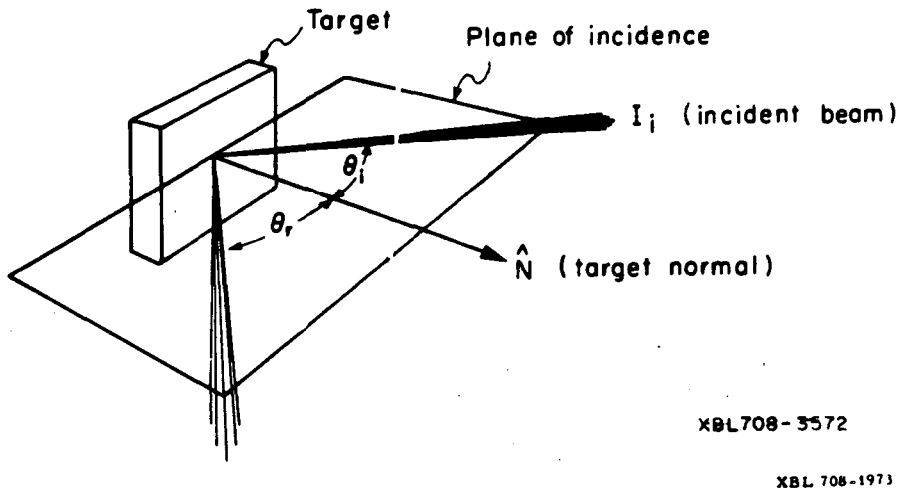

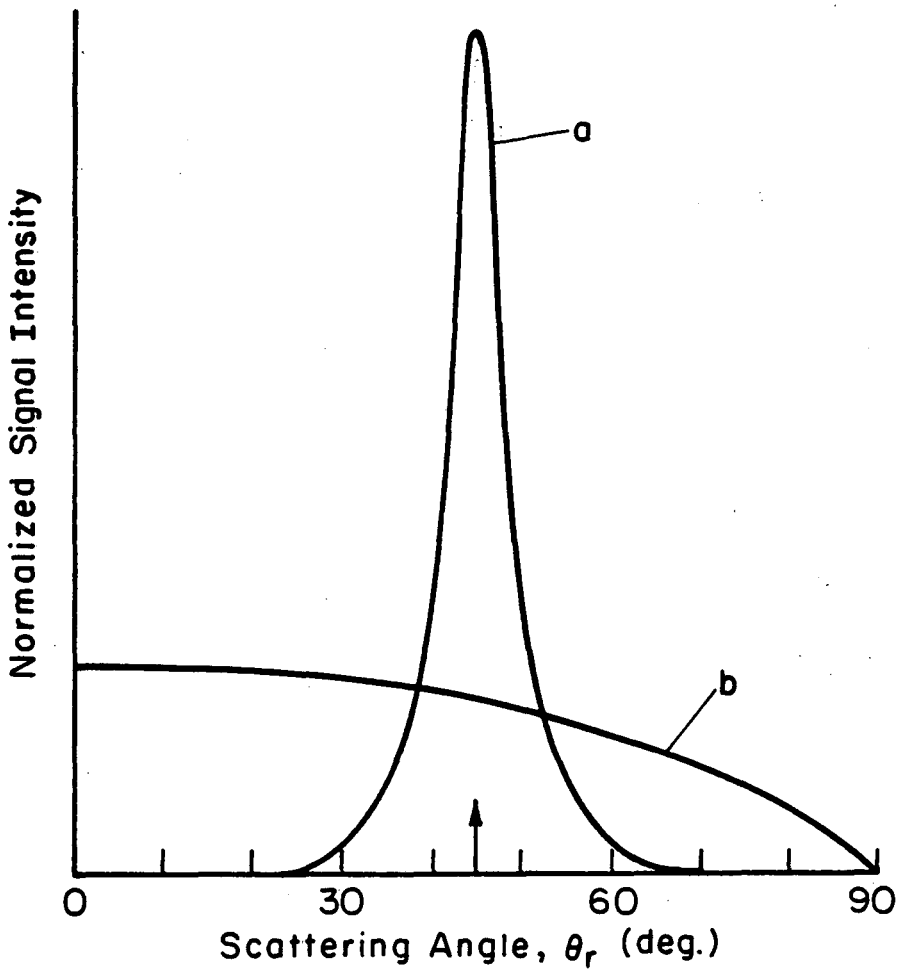

XBL 738-1710

Fig.1

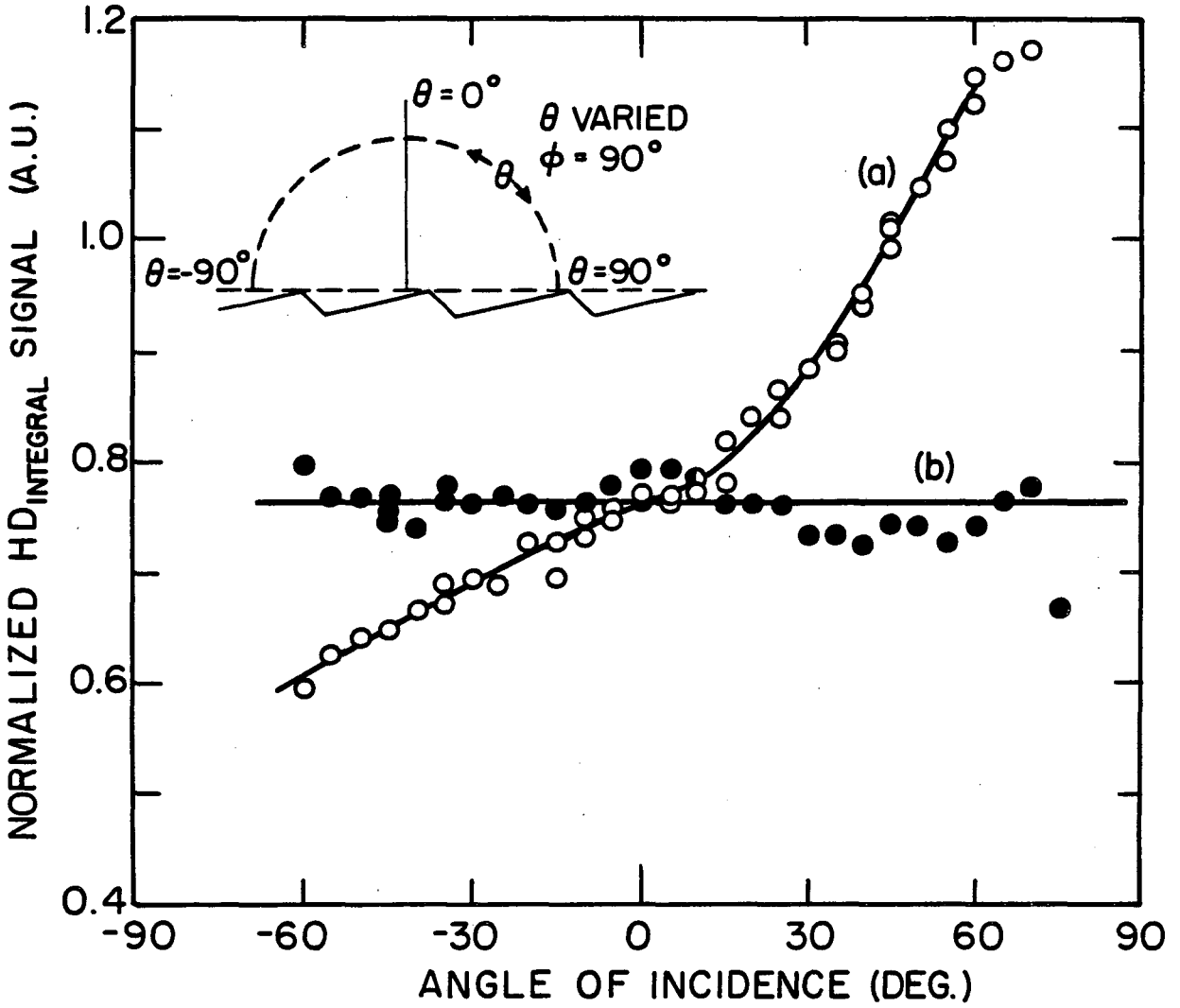

XBL 771-4925

Fig.2

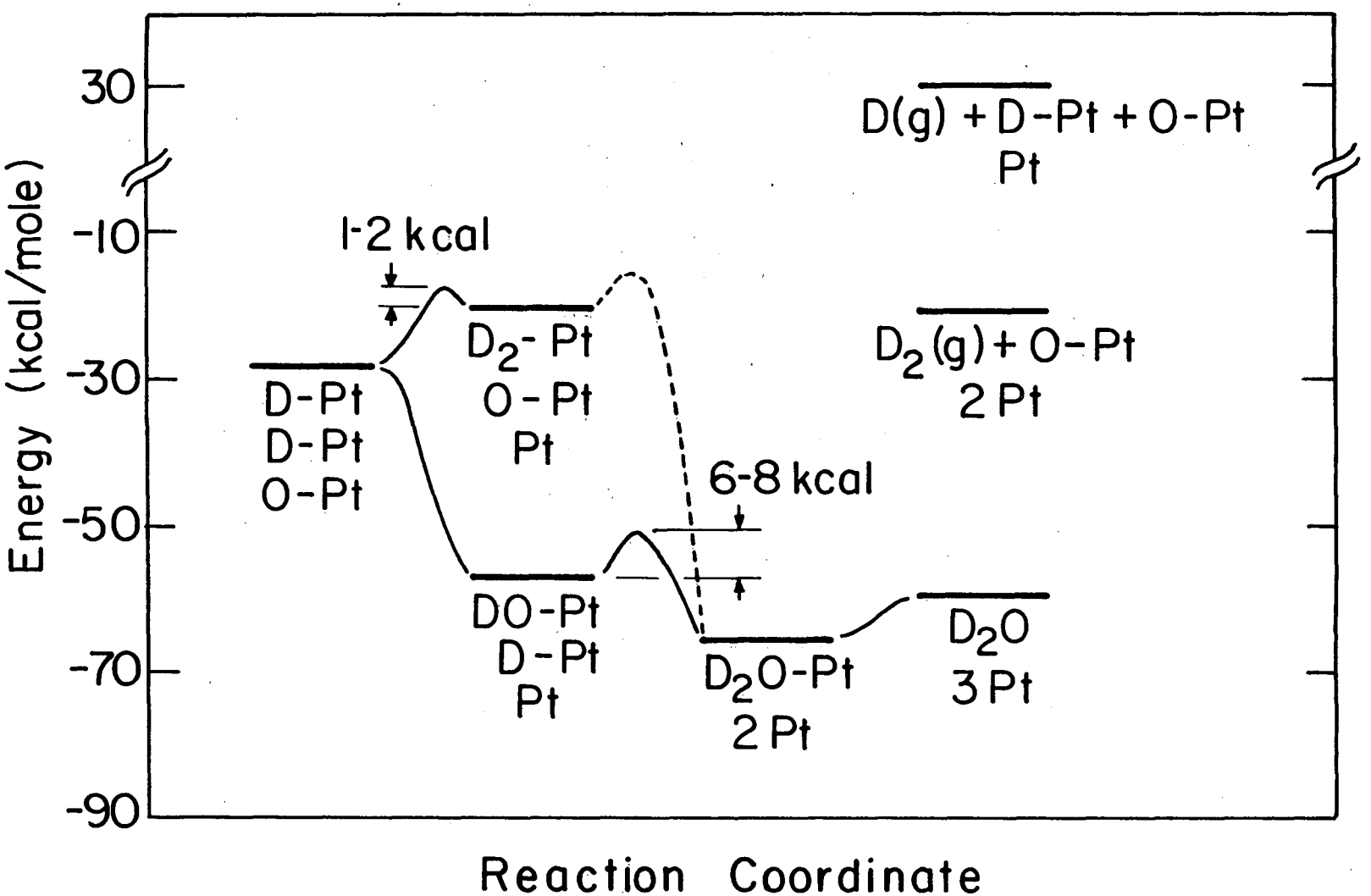

Fig. 3

XBL 813-5386

Table I. Chemical Processes Based on Heterogeneous Catalysis

Processes	Typical Reactions	Catalysts	Reaction Conditions
Ammonia Synthesis	$N_2+3H_2 \rightarrow 2NH_3$	Triply promoted iron (Fe_xO-K_2O-Al_2O_3-CaO); x=0.6-0.9 K promoted Ru	720-800 K 40-100 atm
Ammoxidation	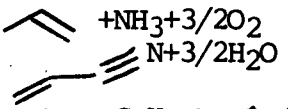 $+NH_3+3/2O_2$ $N+3/2H_2O$	$Bi_2O_3 \cdot MoO_3$, $FeSbO_4$, USb_3O_{10}	670-880 K 1-3 atm
Alkylation	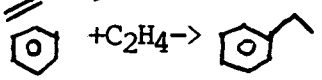 $+C_2H_4 \rightarrow$	solid acids, zeolites	480-580 K 2-5 atm.
Dehydrogenation	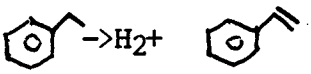 $\rightarrow H_2+$	Fe_2O_3-Cr_2O_3-K_2O mixed metal oxides	800-900 K 10-50 atm.
Epoxidation	$C_2H_4+1/2O_2 \rightarrow C_2H_4O$	AgCl-K_2O/Al_2O_3	520-600 K 10-50 atm.
Fischer-Tropsch synthesis of hydrocarbons	$CO+H_2 \rightarrow$ alkanes olefins aromatics	Fe_3O_4-K_2O/Al_2O_3 supported Co, Ru, Ni, Rh	500-700 K 10-50 atm.
Fischer-Tropsch synthesis of oxygenates	$CO+H_2 \rightarrow$ aldehydes acids alcohols	$Rh_2O_3 \cdot H_2O$-K_2O $LaRhO_4$ supported Pd, Pt	500-700 K 10-50 atm.
Hydrotreating (desulfurization and denitrification)	R-S-R+$H_2 \rightarrow$ 2RH+H_2S R=N-R+3/2H_2 $\rightarrow$ 2RH+NH_3	Co-Mo, Ni-Mo, Ni-Co-Mo/Al_2O_3 Ni-W/Al_2O_3, MoS_2, WS_2	570-770 K 30-200 atm.
Isomerization: olefins	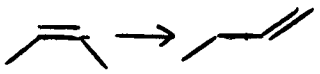	solid acids, zeolites Group VIII metals	270-470 K 1-5 atm
xylenes	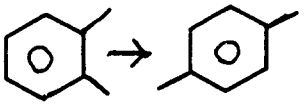	ZSM-5-zeolites	480-580 K 2-5 atm.
alkanes	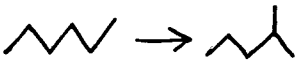	zeolites, Pt/Al_2O_3	570-770 K 5-50 atm.
Methanol synthesis	$CO+2H_2 \rightarrow CH_3OH$	$ZnCrO_3$ ZnO-Cu_2O-Cr_2O_3 ZnO-Cu_2O-Al_2O_3	570-670 K 100-600 atm.
Methanol to gasoline	$CH_3OH \rightarrow$ aromatics olefins, H_2O	ZSM-S zeolites	480-540 K 2-15 atm.

Table I (continued)

Process	Typical Reactions	Catalysts	Reaction Conditions
NO_x Reduction	$NO+5/2H_2 \rightarrow NH_3+H_2O$) $2NO+2H_2 \rightarrow N_2+2H_2O$) $2CO+2NO \rightarrow 2CO_2+N_2$	Ru,Rh,Pd, Pt/SiO_2 Ru,Rh,metal oxides	370-520 K 1-10 atm. 450-650 K 1-10 atm.
Oxidation	olefins) alkanes)$+O_2 \rightarrow CO_2+H_2O$ $2NH_3+5/2O_2 \rightarrow NO+3H_2O$ $CO+1/2O_2 \longrightarrow CO_2$	Group VIII metals	370-670 K 1-10 atm
Oxychlorination	$2HCl+1/2O_2+C_2H_4 \longrightarrow C_2H_4Cl_2$	Cu_2O-CuO/Al_2O_3 metal chlorides	550-700 K 5-30 atm.
Partial oxidation:			
alcohols	$CH_3OH+1/2O_2 \rightarrow H_2CO+H_2O$	Ag, $Fe_2(MoO_4)_3$	550-570 K
o-xylene	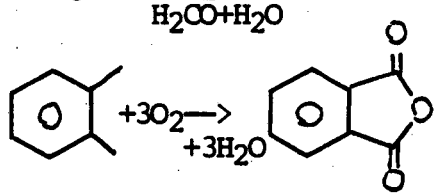	V_2O_5	1-10 atm.
olefins	$C_2H_4+1/2O_2 \longrightarrow CH_3CHO$	V_2O_5	
	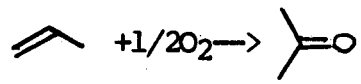	$SnO_2 \cdot MoO_3$	
	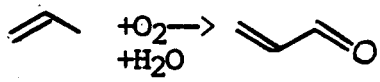	$Bi_2O_3 \cdot MoO_3$	
Reforming:			
Dehydro-generation	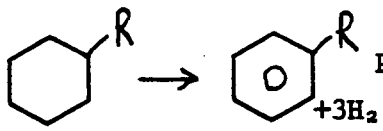	Pt,Pt-Re,Pt-Ge	700-800 K
Dehydro-cyclization	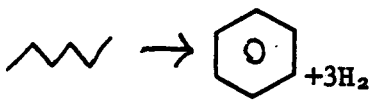	Pt-Au,Pt-Re-Cu	5-50 atm.
Dehydro-isomerization	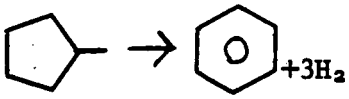	$Ir-Au/Al_2O_3$	
Isomerization	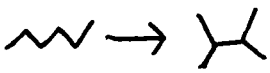		
Hydrogenolysis			
Hydrogenation	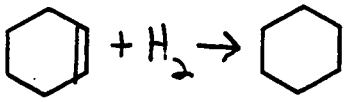		

Table I (continued)

Selective Hydrogenation olefins	H_2 + 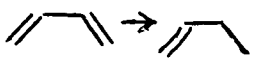	NiS	420-500 K 1-10 atm.
alkynes	R-C ≡ CH+H_2->RHC=CH_2	Pt/Al_2O_3	220-250 K 1-10 atm.
Steam Reforming	$CH_4+H_2O \rightarrow CO+3H_2$	Ni-K_2O/Al_2O_3	850-1100 K 30-100 atm
Water Gas Shift	$CO+H_2O \rightarrow CO_2+H_2$	$Fe_2O_3 \cdot Cr_2O_3$ ZnO-Cu_2O	650-800 K 20-50 atm.
Ziegler-Natta Polymerization	n $C_2H_4 \rightarrow (CH_2-CH_2)_n$	α -$TiCl_3$-$Al(C_2H_5)_2Cl$ Cr_2O_3	~ 370 K 1 atm.

This report was done with support from the Department of Energy. Any conclusions or opinions expressed in this report represent solely those of the author(s) and not necessarily those of The Regents of the University of California, the Lawrence Berkeley Laboratory or the Department of Energy.

Reference to a company or product name does not imply approval or recommendation of the product by the University of California or the U.S. Department of Energy to the exclusion of others that may be suitable.

TECHNICAL INFORMATION DEPARTMENT
LAWRENCE BERKELEY LABORATORY
UNIVERSITY OF CALIFORNIA
BERKELEY, CALIFORNIA 94720